



This is the accepted manuscript made available via CHORUS. The article has been published as:

Focus point in the light stop scenario

A. Delgado, M. Quiros, and C. E. M. Wagner

Phys. Rev. D **90**, 035011 — Published 12 August 2014

DOI: [10.1103/PhysRevD.90.035011](https://doi.org/10.1103/PhysRevD.90.035011)

FOCUS POINT IN THE LIGHT STOP SCENARIO

A. Delgado^a, M. Quiros^b and C. E. M. Wagner^c

*^aDepartment of Physics, University of Notre Dame
Notre Dame, IN 46556, USA*

*^bInstitució Catalana de Recerca i Estudis Avançats (ICREA) and
Institut de Física d'Altes Energies, Universitat Autònoma de Barcelona
08193 Bellaterra, Barcelona, Spain*

*^c Enrico Fermi Institute, Department of Physics and Kavli Institute for
Cosmological Physics, University of Chicago, Chicago, IL 60637, U.S.A.
HEP Division, Argonne National Laboratory, Argonne, IL 60439, U.S.A.*

Abstract

The recent discovery of a light CP-even Higgs in a region of masses consistent with the predictions of models with low energy supersymmetry have intensified the discussion of naturalness in these situations. The focus point solution alleviates the MSSM fine tuning problem. In a previous work, we showed the general form of the MSSM focus point solution, for different values of the messenger scale and of the ratio of gaugino and scalar masses. Here we study the possibility of inducing a light stop as a result of the renormalization group running from high energies. This scenario is highly predictive and leads to observables that may be constrained by future collider and flavor physics data.

1 Introduction

The recent discovery of a Standard Model (SM)-like Higgs boson at the LHC [1, 2], has renewed the interest in weakly coupled extensions of the Standard Model, in which the effects of new physics decouple rapidly as the new physics scale goes above the weak scale. Such models include the minimal supersymmetric extension of the SM (MSSM) [3]. This model includes two Higgs doublets and the lightest CP-even Higgs mass is determined in the limit when the rest of the Higgs spectrum is heavy by the neutral gauge boson mass, M_Z , the ratio of the two vacuum expectation values $\tan\beta$, and the stop mass spectrum. The measured value of the Higgs mass, $m_h \simeq 125$ GeV, may be obtained for moderate or large values of $\tan\beta$ and a stop spectrum at the TeV scale, provided the stop mixing parameter X_t is larger than the average stop mass scale. Larger values of the stop mass scale would be necessary for smaller values of the stop mixing parameter. In particular for small values of X_t and $\tan\beta > 5$, the stop mass scale must be of the order of a few tens of TeV [4–7].

The physical Higgs mass m_h has a logarithmic dependence on the stop mass scale. However the Higgs mass parameter depends on a quadratic way on this scale. Since the Higgs mass parameter must be of order m_h for a proper minimization of the effective Higgs potential, a fine tuning between the tree-level Higgs mass parameter and the radiative corrections must be present. Since the radiative corrections, and therefore the fine tuning, quadratically increase with the stop mass scale, fine tuning arguments lead to the preference of models in which the stops are not heavier than a few TeV and the mixing parameter X_t is sizeable at low energies. Even in the case of stops at the TeV scale, there is the question on the conditions to obtain a Higgs mass parameter at the weak scale when the stop spectrum is of the order of a few TeV, particularly in the case of large messenger scales, in which the radiative corrections to the Higgs mass parameter are increased due to the logarithmic dependence on the messenger scale.

In a previous article [8], we analyzed the general conditions under which the low energy Higgs mass parameter becomes independent of the overall supersymmetric particle mass scale. We call these supersymmetric models generalized focus point (FP) scenarios, since a particular case is the focus point [9–11], in which the scalar masses are universal at the Grand Unification scale M_{GUT} and the gaugino mass parameters are much smaller than the scalar masses. In these models the radiative corrections are not small, but the dependence of the Higgs mass parameter on the boundary value at the messenger scale is appropriately cancelled with the tree-level Higgs mass parameters at the messenger scale. The precise cancellation would, in principle, imply a large fine tuning, since it would imply a precise correlation between the values of the Higgs and stop supersymmetric mass parameters at the messenger scale. The idea behind the focus point is that the necessary correlations occur naturally in specific supersymmetry breaking scenarios, eliminating the need for fine tuning of the mass parameters.

In this article we will analyze the possibility that these correlations could also lead to a light stop in the spectrum in the generalized focus point scenarios. In section 2 we discuss the phenomenological properties of light stops. In section 3 we review the FP solutions and analyze the conditions under which a light stop may be obtained in the spectrum. In

section 4 we discuss particular supersymmetry breaking solutions that lead to Light Stops in FP scenarios. Section 5 will be devoted to our conclusions.

2 Light Stops

As discussed in the previous section, the existence of a focus point in the renormalization group evolution of the Higgs mass parameter allows to raise the supersymmetric particle masses without increasing the low energy value of this parameter. Indeed, the Higgs mass parameter becomes independent of the overall scale of the mass parameters at the messenger scale, and raising the messenger scale values leads to an overall increase of the superpartner masses, without affecting the Higgs mass parameter. However, since the stop masses are affected by similar negative corrections to the ones affecting the Higgs mass parameter, they may be much smaller than the first and second generation squark masses even if they are degenerate at the messenger scale. The presence of light stops is then a generic feature of supersymmetric theories and may lead to interesting phenomenological effects, that may be detected at future experiments.

Direct searches for top superpartners have started to constrain the light stop parameter space [12]. However, depending on how the stop decays, for stop masses above or of the order of 200 GeV, light stops remain unconstrained. In particular if the right handed stop is the lightest squark then the searches are not sensitive in a situation when the lightest chargino or neutralino has a mass difference with the stop smaller than about 50 GeV, since in that case the decay of the stop is a three body decay with soft leptons or jets, making the search quite challenging. Searches for stop production in association with hard jets have started to further restrict this possibility, but currently they loose effectiveness as the stop mass increases beyond 250 GeV. Limits become stronger when there are also light gluinos, with masses below the TeV scale, but in this article we will not consider this possibility.

Within the MSSM, the lightest CP-even Higgs mass is determined via radiative corrections by the stop masses. Therefore both stops can not be at the weak scale, since this would lead to a too small lightest CP-even Higgs mass, in contradiction with the experimentally measured Higgs mass value. Here, we will concentrate on the case in which one of the two stop supersymmetry breaking mass parameter is much smaller than the other one. We will choose m_U to be the smallest stop mass parameter, since it is affected by larger quantum corrections and it is unrelated to the sbottom sector, which is strongly constrained by LHC experimental searches.

The light stops may affect the Higgs phenomenology by modifying the gluon fusion rate [13], [14], [15], [16], [17]. For $m_{Q_L} \gg m_U$, such effects may be suppressed whenever $A_t \simeq m_{Q_L}$. Indeed, the Yukawa coupling of the light stop to the lightest Higgs is approximately given by

$$g_{h\bar{t}t} \simeq h_t^2 v \left(1 - \frac{A_t^2}{m_{Q_L}^2} \right). \quad (2.1)$$

For values of m_{Q_L} of the order of a few TeV and m_U of the order of the weak scale, the

correct Higgs mass is obtained for values of $A_t \gtrsim m_{Q_L}$, implying a small or negative effective Yukawa coupling. Interestingly enough a recent analyses [18, 19] show that for these values of the mixing parameter A_t , which satisfy the trivial condition $A_t^2 < 3 m_{Q_L}^2$ [20, 21], there are no charge and/or color breaking minima deeper than the electroweak minimum, which guarantees the stability of the electroweak vacuum. For the smallest values of $|A_t|$, the Higgs phenomenology is only mildly affected, while for the largest values, the Higgs gluon fusion rate is suppressed, and therefore these values of A_t start to be constrained by current data. These results are shown in Fig. 1, where we have used the program CPsuperH [22] for the computation of the Higgs masses and we have assumed a theoretical error of about 3 GeV in their determination, namely the counters are consistent with $m_h = (125.5 \pm 3)$ GeV. These results differ from the ones presented in Ref. [17] since light staus are absent in the spectrum, implying lower values of $BR(h \rightarrow \gamma\gamma)$ and slightly larger values of the Higgs mass. Values of m_{Q_L} somewhat larger than 2 TeV would make the Higgs phenomenology variations even milder.

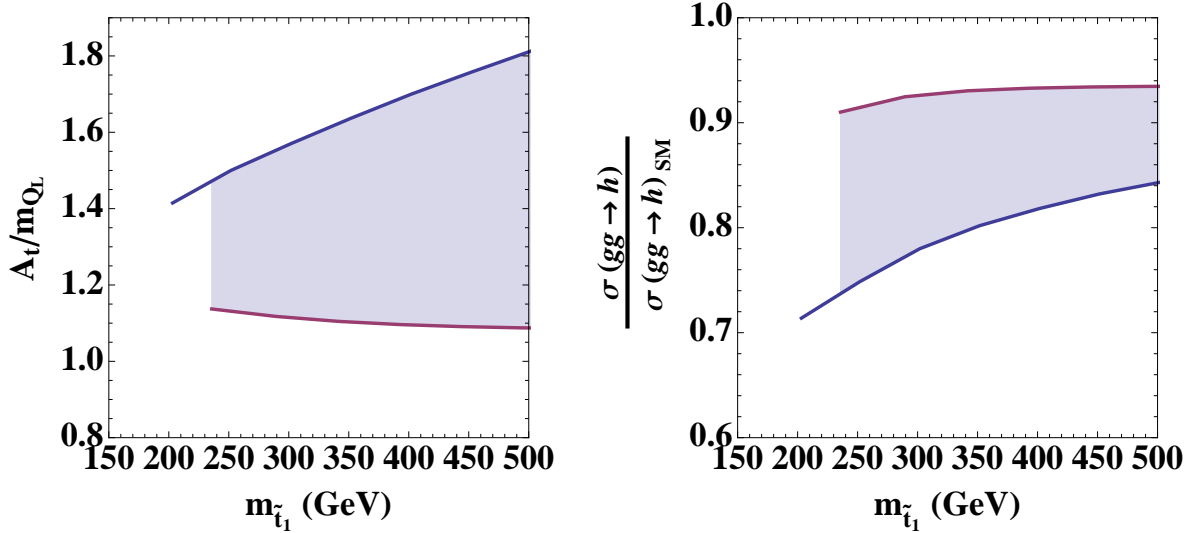


Figure 1: *Left panel* : Values of A_t/m_{Q_L} necessary to reproduce the correct values of the lightest CP-even Higgs mass, $m_h = 125.5 \pm 3$ GeV, as explained in the text, for values of $m_{Q_L} = m_A = 2$ TeV and $\tan \beta = 8$. The value of m_U is varied and remains of the order of the lightest stop mass. *Right panel* : Ratio of the gluon fusion Higgs production rate to the SM value, for the same values of the stop and Higgs mass parameters. Red and blue lines are associated with the smallest and largest allowed values of A_t , respectively.

The gluon fusion suppression is slightly compensated by an enhancement of the diphoton decay rate, which remains larger than in the SM. In the left panel of Fig. 2 we show the total diphoton production rate induced in gluon fusion processes. Flavor processes may also

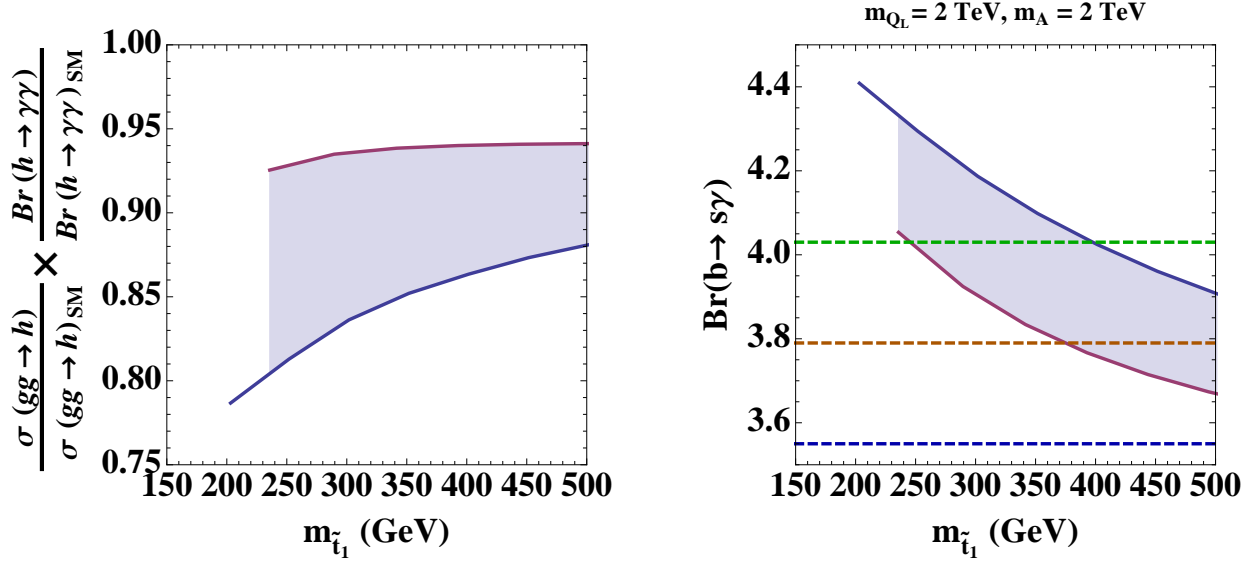


Figure 2: *Left panel: Values of the diphoton production rate for values of $m_{Q_L} = m_A = 2 \text{ TeV}$ and $\tan \beta = 8$. Red and blue lines are associated with the smallest and largest allowed values of A_t , respectively. Right panel: Values of $\text{Br}(b \rightarrow s\gamma)$ obtained for the same values of m_A , m_{Q_L} and A_t as in the left panel. The three lines correspond from top to bottom to the 2σ , σ and the central value of the experimental data.*

be affected by the presence of light stops. Indeed, the amplitude of the decay $b \rightarrow s\gamma$ is affected not only by the presence of light stops but also by the charged Higgs, and possible small flavor violation processes induced by Yukawa coupling effects in the running from high energies. Flavor violation processes may also appear at the messenger scale, induced by the supersymmetry breaking mechanism, but we will ignore these effects. The most important contributions come from the charged Higgs and the stop [23]. The charged Higgs induces a correction to the SM amplitude which is of the same sign as the SM one, but suppressed by the charged Higgs mass squared,

$$\mathcal{A}_{H^+}(b \rightarrow s\gamma) \propto \frac{m_t^2}{m_{H^+}^2}. \quad (2.2)$$

The stop sector, instead, gives a contribution proportional to

$$\mathcal{A}_{\tilde{t}}(b \rightarrow s\gamma) \propto \frac{\mu A_t \tan \beta}{m_{Q_L}^2} \quad (2.3)$$

with a relevant logarithmic dependence on the lightest stop and chargino masses. Large values of $\tan \beta$ would therefore induce large corrections to this process. On the other hand, small values of $\tan \beta$ tend to suppress the Higgs mass. Therefore, moderate values of $\tan \beta \simeq 10$ are preferred in the light stop scenario.

In the right panel of Fig. 2 we show the results for $BR(b \rightarrow s\gamma)$ for $m_{Q_L} = m_A = 2$ TeV and $\tan\beta = 8$, as computed by CPsuperH in the minimal flavor violating scheme for the given hierarchy between the soft breaking parameters induced by the running from high energies. We have chosen $\mu = 200$ GeV, but the results vary only slightly provided μ is not much larger than the weak scale. We also show in the same plot the experimental central value, as well as the values allowed at the one and two σ confidence level. As with the Higgs results, flavor processes allow for a light stop, particularly for the smallest values of A_t consistent with the observed Higgs mass. As it happens with the Higgs observables, somewhat larger values of m_{Q_L} will improve the agreement of the predictions of $BR(b \rightarrow s\gamma)$ with experimental data.

The value of the charged Higgs mass may be estimated by considering the condition of electroweak symmetry breaking. For $m_{H_U}^2 \simeq 0$, obtained in the general FP solution, and moderate or large values of $\tan\beta$, this condition implies a relation between $\tan\beta$, μ and the non-standard Higgs masses, namely

$$\tan^2\beta \simeq \frac{m_{H_D}^2 + \mu^2 + M_Z^2/2}{\mu^2 + m_h^2/2}, \quad (2.4)$$

where the square of the CP-odd mass $m_A^2 \simeq m_{H_D}^2 + 2\mu^2$. Assuming small values of μ , of order of the weak scale, the value of m_{H_D} is naturally of order $\mu \tan\beta$. These large values of m_{H_D} are natural in models of non-universal Higgs masses like the ones we will analyze in the next section. For instance, for values of $\tan\beta \simeq 10$, values of the charged Higgs mass of order of a few TeV are obtained. Such large values of the charged Higgs mass lead only to small corrections to $BR(b \rightarrow s\gamma)$.

In the above, we have concentrated on positive values of A_t . Negative values of A_t make it somewhat more difficult to obtain the observed Higgs mass and, in addition, lead to values of $BR(b \rightarrow s\gamma)$ which are smaller than the 2σ experimental lower bound. However, somewhat larger values of m_{Q_L} would make negative values of A_t consistent with experiment, but we will not explore them in this work.

3 FP in the LSS

Supersymmetry provides a technical solution to the large naturalness problem (i.e. why $v \ll M_P$). However, for large scales of the supersymmetric spectrum \mathcal{Q}_0 , consistent with the non-observation of supersymmetric particles at LHC, an explanation of the little naturalness problem (i.e. why $v \ll \mathcal{Q}_0$) is still required. One particular solution that alleviates the required amount of fine-tuning is if \mathcal{Q}_0 is the generalized FP solution [10] of the running quantity $m_{H_U}^2(\mathcal{Q})$, associated with the requirement that $m_{H_U}^2(\mathcal{Q}_0) = 0$.

On the other hand, as we have discussed before, the experimental bounds on the lightest (mostly right-handed) stop keep room to have a light enough stop, a scenario dubbed LSS as we explained in the introduction. However a mostly right-handed light stop necessarily requires values of the supersymmetric parameter $m_{U_R}^2$ much smaller than the typical supersymmetric scale \mathcal{Q}_0 , thus creating an additional little naturalness problem. A possible

solution to this little hierarchy problem is if \mathcal{Q}_0 is additionally a FP of the running $m_{U_R}^2(\mathcal{Q})$, i.e. if $m_{U_R}^2(\mathcal{Q}_0) \simeq 0$. This can be solved by assuming that $m_{U_R}^2(\mathcal{Q}_0)$ is non zero, but nevertheless its value (as it is small compared to the rest of soft masses) can be neglected in a first approximation. Since in all the region of parameters consistent with the observed Higgs mass and $m_{Q_L}^2(\mathcal{Q}_0) \gg m_{U_R}^2(\mathcal{Q}_0)$, one obtains $m_{t_1}^2 \simeq m_{U_R}^2(\mathcal{Q}_0)$, in practice this amounts to selecting values of m_{U_R} of the order of a few hundred GeV, and much smaller than the characteristic mass parameters at the messenger scale.

In this section we will then deduce the relation on the supersymmetric parameters for \mathcal{Q}_0 to be a double FP characterized by

$$m_{H_U}^2(\mathcal{Q}_0) \simeq m_{U_R}^2(\mathcal{Q}_0) \simeq 0 \quad (3.1)$$

In fact we will consider the strict equality in Eq. (3.1) to make general searches on the parameter space and will introduce small realistic masses $m_{U_R}^2(\mathcal{Q}_0)$ for the particular examples we will present in Sec. 4.

We will assume that the MSSM soft breaking terms (m_{Q_L} , m_{U_R} , M_a , m_{H_U} , m_{H_D} , A_t, \dots) are generated at some high-scale \mathcal{M} , where they are communicated to the observable sector by some messenger fields. We use the notation M_a ($a = 1, 2, 3$) for the Majorana masses of the $SU(3) \otimes SU(2) \otimes U(1)$ gauginos while we reserve the notation Q_L , U_R to the third generation squark fields¹. The value of $m_Q^2(\mathcal{Q})$ for $Q = Q_L, U_R, H_U$ can be computed on general grounds as

$$\begin{aligned} m_Q^2(\mathcal{Q}) = & m_Q^2 + d_Q \left\{ \eta_{Q_L}[\mathcal{Q}, \mathcal{M}] (m_{Q_L}^2 + m_{U_R}^2 + m_{H_U}^2) \right. \\ & + \sum_a \left[\eta_a[\mathcal{Q}, \mathcal{M}] - 2 \left(c_{H_U}^a - \frac{c_Q^a}{d_Q} \right) F_a[\mathcal{Q}, \mathcal{M}] \right] M_a^2 \\ & \left. + \sum_{a \neq b} \eta_{ab}[\mathcal{Q}, \mathcal{M}] M_a M_b + \sum_a \eta_{aA}[\mathcal{Q}, \mathcal{M}] M_a A_t + \eta_A[\mathcal{Q}, \mathcal{M}] A_t^2 \right\} \end{aligned} \quad (3.2)$$

where the functions η_X from the RGE running have been computed semi-analytically in Ref. [24]. In particular by taking the value $\mathcal{Q}_0 = 2$ TeV a fit of the functions $\eta_X[\mathcal{Q}_0, \mathcal{M}]$ was explicitly done in Ref. [8] in a power series of $\log_{10}(\mathcal{M}/\text{GeV})$. The functions F_a are explicitly given by

$$F_a[\mathcal{Q}, \mathcal{M}] = \frac{1}{b_a} \frac{\alpha_a^2(\mathcal{M}) - \alpha_a^2(\mathcal{Q})}{\alpha_a^2(\mathcal{M})} = \frac{\alpha_a(\mathcal{Q})}{2\pi} \log(\mathcal{M}/\mathcal{Q}) \left(2 - \frac{b_a \alpha_a(\mathcal{Q})}{2\pi} \log(\mathcal{M}/\mathcal{Q}) \right) \quad (3.3)$$

where $b_a = (\frac{33}{5}, 1, -3)$ and the coefficients are defined, for $Q = (Q_L, U_R, H_U)$, as

$$c_Q^3 = (4/3, 4/3, 0), \quad c_Q^2 = (3/4, 0, 3/4), \quad c_Q^1 = (1/60, 4/15, 3/20)$$

¹Here we are neglecting the Yukawa couplings h_b and h_τ (as we are never considering too large values of the parameter $\tan\beta$) while the Yukawa couplings of the first two generation are too small and do not play any role.

$$d_Q = (1/3, 2/3, 1) \quad (3.4)$$

Assuming that \mathcal{Q}_0 is the FP defined by $m_{H_U}^2(\mathcal{Q}_0) = 0$, i.e.

$$\begin{aligned} 0 = & m_{H_U}^2 + \eta_{Q_L}[\mathcal{Q}_0, \mathcal{M}](m_{Q_L}^2 + m_{U_R}^2 + m_{H_U}^2) + \sum_a \eta_a[\mathcal{Q}_0, \mathcal{M}]M_a^2 \\ & + \sum_{a \neq b} \eta_{ab}[\mathcal{Q}_0, \mathcal{M}]M_a M_b + \sum_a \eta_{aA}[\mathcal{Q}_0, \mathcal{M}]M_a A_t + \eta_A[\mathcal{Q}_0, \mathcal{M}]A_t^2 \end{aligned} \quad (3.5)$$

one can write the value of $m_{U_R}^2(\mathcal{Q}_0)$ as given by the expression

$$m_{U_R}^2(\mathcal{Q}_0) = m_{U_R}^2 - \frac{2}{3}m_{H_U}^2 + \sum_a c_a M_a^2 F_a[\mathcal{Q}_0, \mathcal{M}] \quad (3.6)$$

where $(c_1, c_2, c_3) = \left(\frac{1}{3}, -1, \frac{8}{3}\right)$. The double FP defined in Eq. (3.1) then requires the condition that

$$m_{U_R}^2 = \frac{2}{3}m_{H_U}^2 - \sum_a c_a M_a^2 F_a[\mathcal{Q}_0, \mathcal{M}] \quad (3.7)$$

The functions F_a then determine when (whether) the LSS FP can be achieved. A plot of them is given in Fig. 3 from where we can see that (by far and depending on the value of

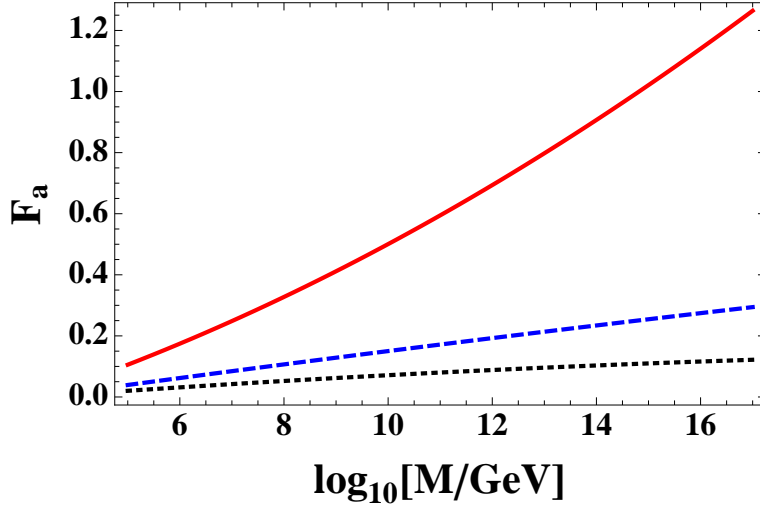


Figure 3: Plots of F_3 (red solid), F_2 (blue dashed) and F_1 (dotted) as functions of $\log_{10}(M/\text{GeV})$.

\mathcal{M}) the main contribution is that coming from the gluino sector.

At the LSS FP we can give the prediction of $m_{Q_L}^2(\mathcal{Q}_0)$ as

$$m_{Q_L}^2(\mathcal{Q}_0) = m_{Q_L}^2 - \frac{1}{2}m_{U_R}^2 + \sum_a d_a M_a^2 F_a[\mathcal{Q}_0, \mathcal{M}] \quad (3.8)$$

where $(d_1, d_2, d_3) = \left(-\frac{7}{30}, \frac{3}{2}, \frac{4}{3}\right)$, while the prediction of $M_a(\mathcal{Q}_0)$ is simply given by

$$M_a(\mathcal{Q}_0) = \frac{\alpha_a(\mathcal{Q}_0)}{\alpha_a(\mathcal{M})} M_a \quad (3.9)$$

Finally and in a similar way we have computed $A_t(\mathcal{Q}_0)$ and made a fit as

$$A_t(\mathcal{Q}_0) = \sum_a \gamma_a(\mathcal{Q}_0, \mathcal{M}) M_a(\mathcal{M}) + \gamma_A(\mathcal{Q}_0, \mathcal{M}) A_t(\mathcal{M}) \quad (3.10)$$

where we use the fit valid for $\mathcal{Q}_0 = 2$ TeV and in the range $\mathcal{M} \in [10^5, 10^{16}]$ GeV

$$\begin{aligned} \gamma_1(\mathcal{Q}_0, \mathcal{M}) &= 0.0149 - 0.0054 y(\mathcal{M}) + 0.0001 y^2(\mathcal{M}) \\ \gamma_2(\mathcal{Q}_0, \mathcal{M}) &= 0.0924 - 0.0336 y(\mathcal{M}) + 0.0008 y^2(\mathcal{M}) \\ \gamma_3(\mathcal{Q}_0, \mathcal{M}) &= 0.3979 - 0.1418 y(\mathcal{M}) + 0.0021 y^2(\mathcal{M}) \\ \gamma_A(\mathcal{Q}_0, \mathcal{M}) &= 1.2576 - 0.1058 y(\mathcal{M}) + 0.0030 y^2(\mathcal{M}), \end{aligned} \quad (3.11)$$

where $y(\mathcal{M}) \equiv \log(\mathcal{M}/\text{GeV})$.

4 Particular Scenarios of Supersymmetry Breaking

In this section we will consider generic cases where the supersymmetry breaking parameters $(m_{Q_L}, m_{U_R}, M_a, m_{H_U}, A_t)$ are such that the double FP equation (3.1) is satisfied. The first (trivial) observation is that in CMSSM-type models characterized by $m_{Q_L} = m_{U_R} = m_{H_U} \equiv m_0$, $M_a \equiv m_{1/2}$ there is no scale \mathcal{Q}_0 satisfying Eq. (3.1). In fact from Eq. (3.7) and given that the sum $c_a F_a[\mathcal{Q}_0, \mathcal{M}] > 0$ (as can be seen from Fig. 3) the condition $m_{U_R}^2 < \frac{2}{3} m_{H_U}^2$ follows. A simple way out is to give up with the degeneracy of m_{U_R} and/or m_{H_U} , as in models dubbed NUHM [25]. This kind of boundary conditions are generic in string constructions [26] where the soft breaking mass of a scalar field is fixed by its modular weight. Non-universal gaugino masses may also be considered [27, 28]. In particular large values of M_2 , that has the negative coefficient in F_2 , Eq. (3.7), can induce positive corrections to the Higgs mass parameter without affecting the right-handed stop mass parameter, making it possible to fulfill the double FP condition even for universal scalar masses. However, since very large values of M_2 would be required for this to happen, and string constructions provide, at tree level, universal gaugino masses, we will only concentrate in the following on the case of non-universal scalar masses.

4.1 Non-Universal Higgs Masses

We will consider the supersymmetric parameters where at the messenger scale the Higgs sector has a different mass from the one of the squark-slepton sector, namely the four independent parameters at the scale \mathcal{M} are

$$m_{Q_L} = m_{U_R} \equiv m_0, \quad A_t, \quad m_{H_U} = m_{H_D} \equiv m_H, \quad M_a \equiv m_{1/2} \quad (4.1)$$

and will impose the double FP condition for \mathcal{Q}_0 as in Eq. (3.1). The results are shown in Figs. 4 and 5.

In the left panel of Fig. 4 we show contour lines of constant $m_{1/2}/m_H$ (solid lines) and

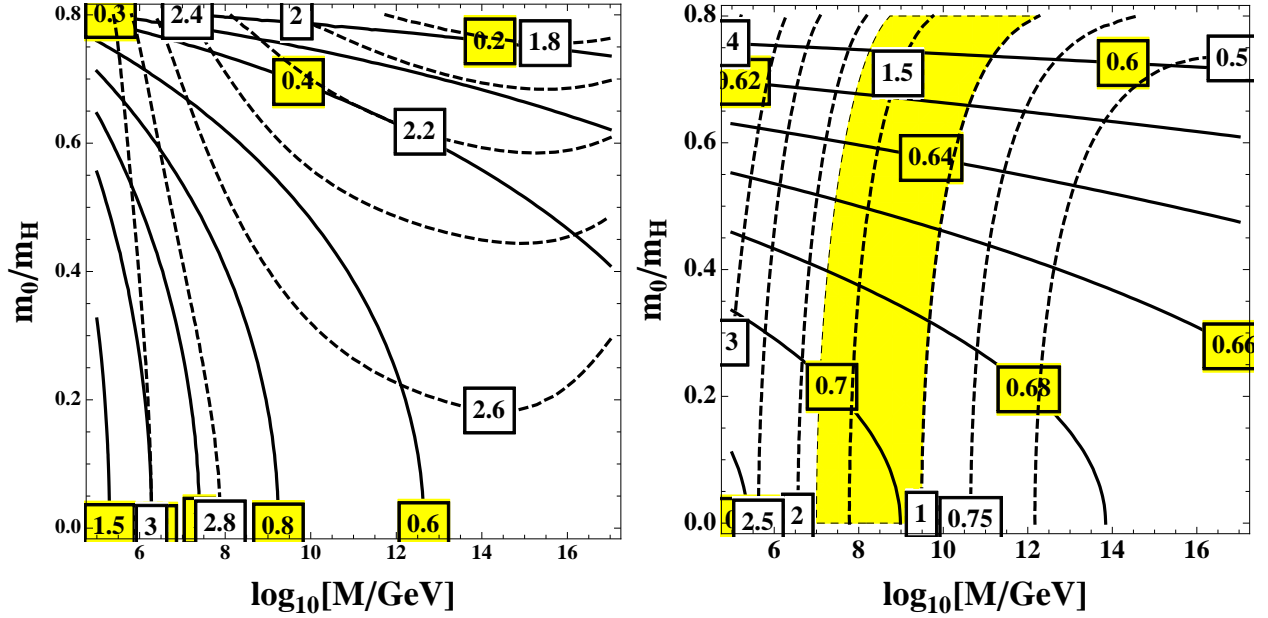


Figure 4: *Left panel: Solid (dashed) lines are contour lines of $m_{1/2}/m_H$ (A_t/m_H for $A_t > 0$) in the plane $(\log_{10}[\mathcal{M}/\text{GeV}], m_0/m_H)$. Right panel: Solid (dashed) lines are contour lines of $m_{Q_L}(\mathcal{Q}_0)/m_H$ ($A_t(\mathcal{Q}_0)/m_{Q_L}(\mathcal{Q}_0)$ for $A_t(\mathcal{Q}_0) > 0$) in the plane $(\log_{10}[\mathcal{M}/\text{GeV}], m_0/m_H)$. Shadowed region corresponds to $1 \lesssim A_t(\mathcal{Q}_0)/m_{Q_L}(\mathcal{Q}_0) \lesssim 1.8$.*

A_t/m_H in the plane $[\log(\mathcal{M}/\text{GeV}), m_0/m_H]$ where we only consider the region where $A_t > 0$ in agreement with the results from Sec. 2. In fact we can see that there is an upper bound $m_0^2/m_H^2 \leq 2/3$ which is reached for massless gauginos $m_{1/2}/m_H = 0$. A particular realization of a model with $m_0^2 \simeq 2/3 m_H^2$ and $m_{1/2} \ll m_H$, was proposed in Ref. [29], where the heavy scalars are generated by gauge mediation of an extra $U(1)_\chi \otimes U(1)_F$ group spontaneously broken at high scales, while the masses of light gauginos are generated by gravity mediation.

More important for phenomenological purposes are the values of supersymmetric parameters at the scale \mathcal{Q}_0 . In the right panel of Fig. 4 we show contour lines of $m_{Q_L}(\mathcal{Q}_0)/m_H$ (solid lines) and of $A_t(\mathcal{Q}_0)/m_{Q_L}(\mathcal{Q}_0)$ (dashed lines). In particular we can see that the (shadowed) region $1 \lesssim A_t(\mathcal{Q}_0)/m_{Q_L}(\mathcal{Q}_0) \lesssim 1.8$ allowed by the Higgs mass determination is consistent with scales $10^7 \text{ GeV} \lesssim \mathcal{M} \lesssim 10^{12} \text{ GeV}$. In this region we see that there is a window of values of $m_{Q_L}(\mathcal{Q}_0)$ as $0.6 \lesssim m_{Q_L}(\mathcal{Q}_0)/m_H \lesssim 0.7$. As for the values of $M_a(\mathcal{Q}_0)/m_{Q_L}(\mathcal{Q}_0)$ they are plotted in the left panel of Fig. 5 for $M_3(\mathcal{Q}_0)$ (solid lines), and in the right panel of Fig. 5 for $M_2(\mathcal{Q}_0)$ (dashed lines) and for $M_1(\mathcal{Q}_0)$ (dotted lines). In particular in the selected region the gluino mass is in the window $0.5 \lesssim M_3(\mathcal{Q}_0)/m_{Q_L}(\mathcal{Q}_0) \lesssim 2$. In all cases the band allowed by the Higgs mass is superimposed in the contour plots of supersymmetric parameters at

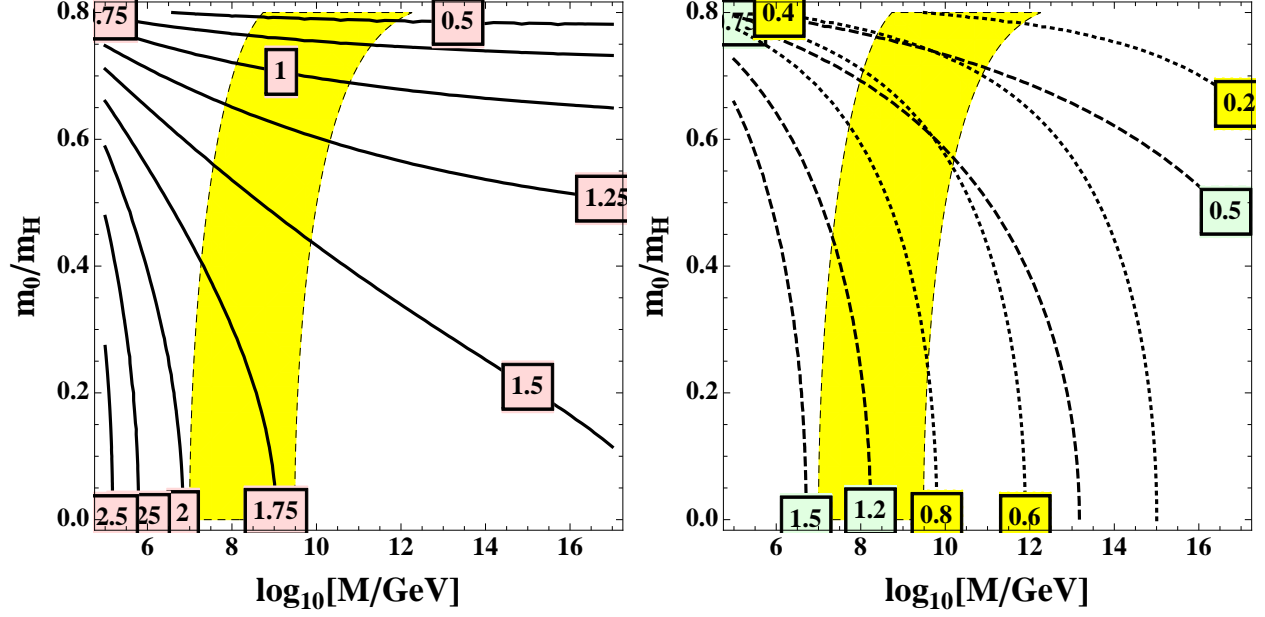


Figure 5: *Left panel: Contour lines of $M_3(\mathcal{Q}_0)/m_{Q_L}(\mathcal{Q}_0)$ in the plane $(\log_{10}[\mathcal{M}/\text{GeV}], m_0/m_H)$. Right panel: Contour lines of $M_2(\mathcal{Q}_0)/m_{Q_L}(\mathcal{Q}_0)$ (dashed lines) and $M_1(\mathcal{Q}_0)/m_{Q_L}(\mathcal{Q}_0)$ (dotted lines) in the plane $(\log_{10}[\mathcal{M}/\text{GeV}], m_0/m_H)$. Shaded region corresponds to $1 \lesssim A_t(\mathcal{Q}_0)/m_{Q_L}(\mathcal{Q}_0) \lesssim 1.8$.*

the low scale \mathcal{Q}_0 .

As a simple estimate and to get a feeling of the order of magnitude of the involved parameters we will fix $m_{Q_L}(\mathcal{Q}_0) \simeq 2$ TeV which is achieved in the selected region for

$$2.9 \text{ TeV} \lesssim m_H \lesssim 3.3 \text{ TeV}, \quad 0 < m_0 \lesssim 2.5 \text{ TeV} \quad (4.2)$$

and then implies that

$$\begin{aligned} 2 \text{ TeV} &\lesssim A_t(\mathcal{Q}_0) \lesssim 3.6 \text{ TeV} \\ 1.5 \text{ TeV} &\lesssim M_3(\mathcal{Q}_0) \lesssim 4 \text{ TeV} \\ 700 \text{ GeV} &\lesssim M_2(\mathcal{Q}_0) \lesssim 3 \text{ TeV} \\ 500 \text{ GeV} &\lesssim M_1(\mathcal{Q}_0) \lesssim 2.5 \text{ TeV} \end{aligned} \quad (4.3)$$

where we have constrained $m_0 \lesssim 0.75 m_H$ to not have too light gluino masses. A particular case ² is given in Tab. 1 where the messenger scale $\mathcal{M} = 10^{10}$ GeV is selected and the input parameters at the messenger scale are given in the left side of Tab. 1 while the output parameters at the scale \mathcal{Q}_0 are given on its right side. We have also used as an input parameter, in Eq. (3.6), $m_{U_R}^2(\mathcal{Q}_0) = 0.02 m_H^2$. If we fix $m_{Q_L}(\mathcal{Q}_0) = 2$ TeV it corresponds

²In this and in the next examples we have considered realistic values $200 \text{ GeV} \lesssim m_{U_R}(\mathcal{Q}_0) \lesssim 500 \text{ GeV}$, as we will specify.

$\frac{m_0}{m_H}$	$\frac{A_t}{m_H}$	$\frac{m_{1/2}}{m_H}$	$\frac{m_{Q_L}(\mathcal{Q}_0)}{m_H}$	$\frac{m_{U_R}(\mathcal{Q}_0)}{m_{Q_L}(\mathcal{Q}_0)}$	$\frac{A_t(\mathcal{Q}_0)}{m_{Q_L}(\mathcal{Q}_0)}$	$\frac{M_3(\mathcal{Q}_0)}{m_{Q_L}(\mathcal{Q}_0)}$	$\frac{M_2(\mathcal{Q}_0)}{m_{Q_L}(\mathcal{Q}_0)}$	$\frac{M_1(\mathcal{Q}_0)}{m_{Q_L}(\mathcal{Q}_0)}$
0.6	2.35	0.52	0.65	0.22	1.03	1.27	0.74	0.59

Table 1: A particular set of parameters at $\mathcal{M} = 10^{10}$ GeV (left set) and low \mathcal{Q}_0 energy (right set) from Figs. 4 and 5.

to $m_{U_R}(\mathcal{Q}_0) \simeq 440$ GeV, $m_H \simeq 3.1$ TeV and $m_0 \simeq 1.9$ TeV, $m_{1/2} \simeq 1.6$ TeV, $A_t \simeq 7.5$ TeV. On the other hand the gluino and electroweak gaugino low energy masses $M_a(\mathcal{Q}_0)$ are (2.52, 1.48, 1.18) TeV, for $a = 3, 2, 1$, respectively.

4.2 Non-Universal Scalar Masses

As we have seen in the previous section from the double FP condition, in view of the current experimental constraints on the Higgs and gluino masses, the transmission of supersymmetry breaking at the GUT scale $\mathcal{M}_{GUT} \simeq 2 \times 10^{16}$ GeV cannot be achieved for non-universal Higgs masses and universal gaugino masses. A way out is to give up the universality of the squark masses, a generic situation which appears on soft breaking terms coming from superstring theories [26]. Therefore in this section we will consider soft breaking terms characterized by the five independent parameters defined at the unification scale \mathcal{M}_{GUT}

$$m_{Q_L}, \quad m_{U_R}, \quad A_t, \quad m_{H_U} \equiv m_H, \quad M_a \equiv m_{1/2} \quad (4.4)$$

on which we will impose the double FP condition (3.7). The results are shown in Figs. 6 and 7. This kind of boundary condition could potentially produce a non-zero Fayet-Iliopoulos (FI) term in the RGE evolutions of soft masses. As its impact on the present calculation is proportional to g_1^2 and therefore tiny, we are going to assume in the remaining of this subsection that the rest of scalar masses are such that the FI cancels.

In the left panel of Fig. 6 we show contour lines of m_{Q_L}/m_H (solid lines) and m_{U_R}/m_H (dashed lines) in the plane $(m_{1/2}/m_H, A_t/m_H)$ and, as we did in the previous section, we have selected positive values $A_t > 0$, in agreement with phenomenological requirements on the LSS as we showed in Sec. 2. Contour lines for $m_{Q_L}(\mathcal{Q}_0)/m_H$ are shown in the right panel of Fig. 6 (dotted lines) along with the contours of $A_t(\mathcal{Q}_0)/m_{Q_L}(\mathcal{Q}_0) = 1$ (lower solid line) and $A_t(\mathcal{Q}_0)/m_{Q_L}(\mathcal{Q}_0) = 1.8$ (upper solid line) such that the available region which can accommodate the experimental value of the Higgs mass is the shadowed (yellow) region.

Contour plots for $M_a(\mathcal{Q}_0)/m_{Q_L}(\mathcal{Q}_0)$ are exhibited in Fig. 7. In particular in the left panel contour lines of the gluino mass ratio $M_3(\mathcal{Q}_0)/m_{Q_L}(\mathcal{Q}_0)$ (solid lines) are presented while the electroweak gaugino mass ratios are exhibited in the right panel for $M_2(\mathcal{Q}_0)/m_{Q_L}(\mathcal{Q}_0)$ (dashed lines) and for $M_1(\mathcal{Q}_0)/m_{Q_L}(\mathcal{Q}_0)$ (dotted lines). In all cases the region where the theory is consistent with the Higgs mass is superimposed with the other contour lines.

Two typical examples are provided in Tabs. 2 and 3 where we present sets of input parameters in units of m_H , at the scale \mathcal{M}_{GUT} (left side of tables) and the corresponding output parameters at the scale \mathcal{Q}_0 (right side of tables). We have fixed here $m_{U_R}^2(\mathcal{Q}_0) = 0.005 m_H^2$.

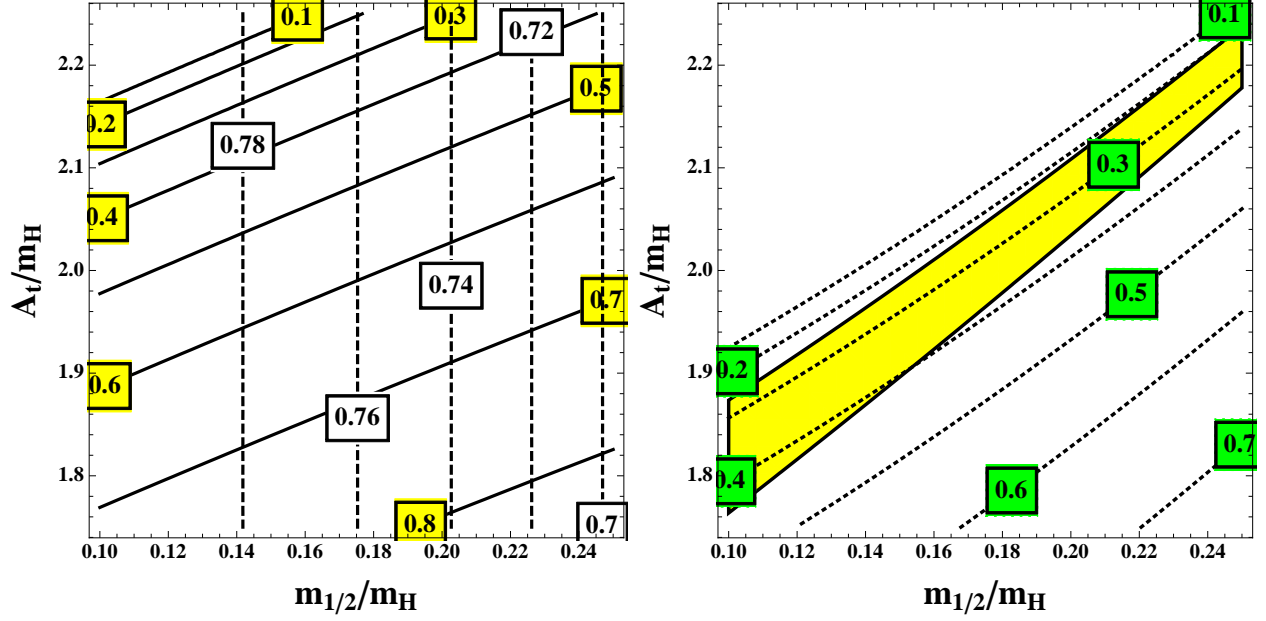


Figure 6: Contour lines for $\mathcal{M}_{GUT} = 2 \times 10^{16}$ GeV. Left panel: Solid (dashed) lines are contour lines of m_{Q_L}/m_H (m_{U_R}/m_H) in the plane $(m_{1/2}/m_H, A_t/m_H)$. Right panel: Solid lines are contour lines for $A_t(Q_0)/m_{Q_L}(Q_0) = 1$ (lower line) and 1.8 (upper line). Shaded region is allowed by the Higgs mass. Dotted lines are contour lines for $m_{Q_L}(Q_0)/m_H$ in the plane $(m_{1/2}/m_H, A_t/m_H)$.

The model in Tab. 2 corresponds to heavy gauginos while that in Tab. 3 corresponds to lighter gauginos. In fact fixing $m_{Q_L}(Q_0) = 2$ TeV amounts then to $m_H \simeq 6$ TeV, and $m_{U_R}(Q_0) \simeq 440$ GeV for the case of Tab. 2 and $m_H \simeq 5$ TeV, and $m_{U_R}(Q_0) \simeq 360$ GeV for the case of Tab. 3. The gaugino masses at the low scale $M_a(Q_0)$ are given by (2.84, 1.14, 0.64) TeV, for $a = 3, 2, 1$ respectively, for the case of Tab. 2, and (1.4, 0.56, 0.30) TeV, for $a = 3, 2, 1$ respectively, for the case of Tab. 3.

4.3 Electroweak Symmetry Breaking and the Charged Higgs Mass

The value of m_{H_D} at the low scale Q_0 has to satisfy the EoM, Eq. (2.4), which leads to $m_{H_D}(Q_0) \simeq \tan \beta \mu(Q_0)$. As the value of m_{H_D} at the high scale \mathcal{M} does decouple from the

$\frac{m_{1/2}}{m_H}$	$\frac{A_t}{m_H}$	$\frac{m_{Q_L}}{m_H}$	$\frac{m_{U_R}}{m_H}$	$\frac{m_{Q_L}(Q_0)}{m_H}$	$\frac{m_{U_R}(Q_0)}{m_{Q_L}(Q_0)}$	$\frac{A_t(Q_0)}{m_{Q_L}(Q_0)}$	$\frac{M_3(Q_0)}{m_{Q_L}(Q_0)}$	$\frac{M_2(Q_0)}{m_{Q_L}(Q_0)}$	$\frac{M_1(Q_0)}{m_{Q_L}(Q_0)}$
0.22	2.1	0.55	0.73	0.33	0.22	1.08	1.42	0.57	0.32

Table 2: One particular set of parameters at high (\mathcal{M}_{GUT}) and low (Q_0) energy from Figs. 6 and 7 leading to heavy electroweak gauginos.

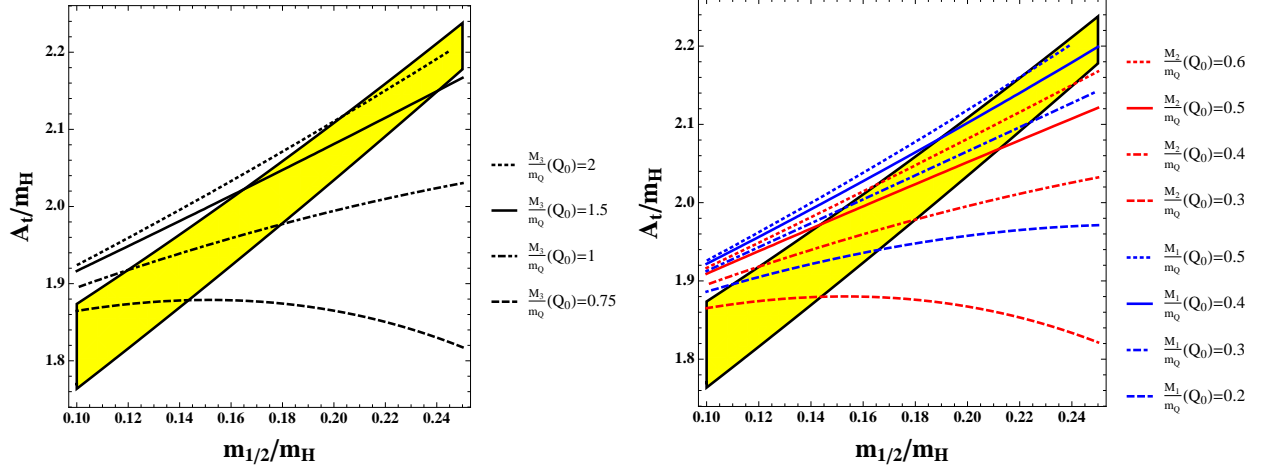


Figure 7: Contour lines for $\mathcal{M}_{GUT} = 2 \times 10^{16}$ GeV. Left panel: Contour lines of gluino mass ratios $M_3(\mathcal{Q}_0)/m_{Q_L}(\mathcal{Q}_0)$ in the plane $(m_{1/2}/m_H, A_t/m_H)$. Right panel: Contour lines of electroweak gaugino mass ratios $M_2(\mathcal{Q}_0)/m_{Q_L}(\mathcal{Q}_0)$ and $M_1(\mathcal{Q}_0)/m_{Q_L}(\mathcal{Q}_0)$ in the plane $(m_{1/2}/m_H, A_t/m_H)$. The allowed region by the Higgs mass is superimposed.

$\frac{m_{1/2}}{m_H}$	$\frac{A_t}{m_H}$	$\frac{m_{Q_L}}{m_H}$	$\frac{m_{U_R}}{m_H}$	$\frac{m_{Q_L}(\mathcal{Q}_0)}{m_H}$	$\frac{m_{U_R}(\mathcal{Q}_0)}{m_{Q_L}(\mathcal{Q}_0)}$	$\frac{A_t(\mathcal{Q}_0)}{m_{Q_L}(\mathcal{Q}_0)}$	$\frac{M_3(\mathcal{Q}_0)}{m_{Q_L}(\mathcal{Q}_0)}$	$\frac{M_2(\mathcal{Q}_0)}{m_{Q_L}(\mathcal{Q}_0)}$	$\frac{M_1(\mathcal{Q}_0)}{m_{Q_L}(\mathcal{Q}_0)}$
0.13	1.85	0.66	0.79	0.40	0.18	1.05	0.70	0.28	0.15

Table 3: Another particular set of parameters at high (\mathcal{M}_{GUT}) and low (\mathcal{Q}_0) energy from Figs. 6 and 7 leading to lighter electroweak gauginos.

one-loop calculation of the double FP condition, and as it renormalizes by a little amount because of the bottom Yukawa and electroweak gauge couplings we can assume the relation $m_{H_D} \simeq \tan \beta \mu$ which can then be used to fix m_{H_D} or μ .

Imposing the cancellation of the hypercharge FI D-term contribution, the soft supersymmetry breaking parameter $m_{H_D}^2$ may be determined as a function of the other scalar mass parameters

$$m_{H_D}^2 = 3 (m_{Q_L}^2 - 2 m_{U_R}^2 + m_{D_R}^2 - m_{L_L}^2 + m_{E_R}^2) + m_{H_U}^2, \quad (4.5)$$

where the factor 3 comes from the number of generations and we have assumed flavor universality. For simplicity, we will assume that the mass difference in the slepton sector is zero or small compared to the ones appearing in the squark and Higgs sector. In such a case, m_{H_D} is simply determined as a function of m_{H_U} and the squark mass parameters.

As an example, let us assume that $m_{D_R}^2 = m_{U_R}^2$. Then,

$$\frac{m_{H_D}^2}{m_{H_U}^2} = 3 \left(\frac{m_{Q_L}^2}{m_{H_U}^2} - \frac{m_{U_R}^2}{m_{H_U}^2} \right) + 1. \quad (4.6)$$

Since in the LSS at the messenger scale $m_{Q_L} < m_{U_R}$, one obtains a reduction of m_{H_D} with respect to m_{H_U} . For instance, if one takes the values of the parameters displayed in the upper right corner of the yellow shaded region in Fig. 6, $m_{Q_L} = 0.45m_H$ and $m_{U_R} = 0.7m_H$, we obtain

$$\frac{m_{H_D}^2}{m_{H_U}^2} \simeq 0.1. \quad (4.7)$$

Since $m_H/m_{Q_L}(\mathcal{Q}_0) \simeq 5$ then m_H is of order 10 TeV and m_{H_D} and the charged Higgs mass would be of order 3 TeV. Eq. (4.6) leads to similar values of the charged Higgs mass obtained throughout the yellow shaded region in Fig. 6.

If, instead, we assumed that $m_{D_R} = m_{Q_L}$, then the values of the charged Higgs mass become smaller, and consistent solutions, without tachyons, may only be obtained for small values of the gaugino masses in Fig. 6. These examples simply show that for reasonable boundary conditions of the scalar mass parameters, the condition of cancellation of the FI term tends to induce values of the charged Higgs mass that are of order $m_{Q_L}(\mathcal{Q}_0)$, significantly smaller than m_H . This, in turn, is consistent with the condition of electroweak symmetry breaking for small values of μ and moderate values of $\tan\beta$, and as we show in section 2, may lead to agreement with collider and flavor constraints in the LSS.

4.4 Lightest Neutralino, Dark Matter and Stop Searches

Quite generally, in the generalized focus point scenario, the value of μ is small and then the lightest neutralino has a significant Higgsino component. Light Higgsinos lead to a thermal relic density that is far smaller than the one observed experimentally and therefore either non-thermal production or other sources of Dark-Matter are required in this case.

If Higgsinos are the only particle lighter than the light stop, then the stop would tend to decay into a bottom quark and a charged Higgsino. The charged Higgsino, in turn, would decay into a neutral Higgsino and soft quarks and leptons, which would be difficult to observe at the LHC. Therefore, at the LHC stop decays would lead to bottom quarks and missing energy and therefore standard sbottom searches (with sbottoms decaying into bottom quark and missing energy) may be used to constrain this scenario [30]. Stop masses within a few tens of GeV of the neutralino mass would remain unconstrained in this case.

In certain cases, the gaugino masses are small and then a thermal Dark Matter may be obtained with a well tempered neutralino condition [31]. For instance, Table 3 present a case in which the Bino mass is of order 300 GeV and naturally of order μ . In general, M_1 has only a small impact on the renormalization group evolution of the scalar mass parameters and therefore the value of M_1 may be lowered without affecting the general properties of the FP solution. Direct Dark Matter detection mediated by the CP-even Higgs bosons put constraints on this scenario, which become weaker for negative values of M_1 [32–35]. On the other hand, in such a case the mass difference between charginos and neutralinos become larger than in the light Higgsino scenario and searches for stops proceed in the standard $b + W + \text{Missing Energy}$ channel that we discussed in Sec. 2.

5 Conclusions

In this article we have discussed the possibility of obtaining a double focus point, light stop scenario, in which both the right-handed stop mass parameter $m_{U_R}^2$ and the Higgs mass parameter $m_{H_U}^2$ become independent of the generic supersymmetric particle mass scale. We have required the gluino to be heavy and a stop mixing parameter A_t such that the right Higgs mass is obtained without affecting in a drastic way the Higgs phenomenology. For this to happen, the low energy mixing parameter should be of the order or somewhat larger than the heaviest stop mass, namely $A_t(Q_0) \gtrsim m_{Q_L}(Q_0)$.

The requirement of obtaining a light stop within the focus point scenario demands particular correlations of the scalar and gaugino mass parameters at the messenger scale. In particular, this cannot be achieved in the case of universal scalar and gaugino masses. We have shown, however, that a double focus fixed point may be achieved in the case of non-universal Higgs mass parameters. Even in such a case, the LSS demands a messenger scale significantly smaller than the GUT scale $\mathcal{M}_{GUT} \simeq 2 \times 10^{16}$ GeV.

In view of these constraints, we have studied the conditions under which a light stop may be obtained with a messenger scale of the order of the GUT scale. Concentrating on the case of universal gaugino masses, we have determined the specific scalar mass parameter correlations that lead to the presence of a double focus point within the LSS. For this to happen, for not too heavy gluino masses, the scalar mass parameters at the GUT scale must remain of the same order, but they must fulfill specific correlations, namely, $m_{U_R}^2/m_{H_U}^2 \lesssim 0.65$, and $m_{Q_L}^2/m_{H_U}^2 \lesssim 0.5$, while the mixing parameter, $1.5 m_{H_U} \lesssim A_t \lesssim 2.5 m_{H_U}$. Finally, the universal gaugino masses should acquire moderate values, $m_{1/2} \lesssim 0.3 m_{H_U}$.

We have also shown that the condition of electroweak symmetry breaking demands the CP-odd Higgs boson mass $m_A \simeq \mu \tan \beta$. For low energy values of $m_{Q_L}(Q_0)$ of a few TeV, moderate values of $\tan \beta$ are required in order to obtain the proper Higgs mass while keeping agreement with flavor physics constraints, in particular the measured value of the $BR(b \rightarrow s\gamma)$. For the specific non-universal scalar masses analyzed in this article, the value of $m_{H_D}^2$ at the messenger scale must be smaller than $m_{H_U}^2$, what can be obtained in simple supersymmetry breaking scenarios.

Acknowledgments

The work of AD was partially supported by the National Science Foundation under grant PHY-1215979. The work of MQ was supported in part by the European Commission under the ERC Advanced Grant BSMOXFORD 228169, by the Spanish Consolider-Ingenio 2010 Programme CPAN (CSD2007-00042), by CICYT-FEDER-FPA2011-25948 and by Secretaria d'Universitats i Recerca del Departament d'Economia i Coneixement de la Generalitat de Catalunya under Grant number 2014 SGR 1450. The work of CW at ANL is supported in part by the U.S. Department of Energy under Contract No. DE-AC02-06CH11357.

References

- [1] **ATLAS** Collaboration, “ATLAS SUSY 2013 Summary”
https://twiki.cern.ch/twiki/pub/AtlasPublic/CombinedSummaryPlots/AtlasSearchesSUSY_SUSY2013.pdf.
- [2] **CMS** Collaboration, “CMS SUSY 2013 Summary”
https://twiki.cern.ch/twiki/pub/CMSPublic/SUSYSMSSummaryPlots8TeV/barplot_blue_orange_SUSY2013.pdf.
- [3] H. P. Nilles, “Supersymmetry, Supergravity And Particle Physics,” Phys. Rept. **110** (1984) 1; H. E. Haber and G. L. Kane, “The Search For Supersymmetry: Probing Physics Beyond The Standard Model,” Phys. Rept. **117** (1985) 75; S. P. Martin, “A supersymmetry primer,” arXiv:hep-ph/9709356.
- [4] M. E. Cabrera, J. A. Casas and A. Delgado, “Upper Bounds on Superpartner Masses from Upper Bounds on the Higgs Boson Mass,” Phys. Rev. Lett. **108**, 021802 (2012) [arXiv:1108.3867 [hep-ph]]; G. F. Giudice and A. Strumia, “Probing High-Scale and Split Supersymmetry with Higgs Mass Measurements,” Nucl. Phys. B **858**, 63 (2012) [arXiv:1108.6077 [hep-ph]].
- [5] T. Hahn, S. Heinemeyer, W. Hollik, H. Rzehak and G. Weiglein, “High-precision predictions for the light CP-even Higgs Boson Mass of the MSSM,” Phys. Rev. Lett. **112**, 141801 (2014) [arXiv:1312.4937 [hep-ph]].
- [6] A. Delgado, M. Garcia and M. Quiros, “Electroweak and supersymmetry breaking from the Higgs discovery,” arXiv:1312.3235 [hep-ph].
- [7] P. Draper, G. Lee and C. E. M. Wagner, “Precise Estimates of the Higgs Mass in Heavy SUSY,” Phys. Rev. D **89**, 055023 (2014) [arXiv:1312.5743 [hep-ph]].
- [8] A. Delgado, M. Quiros and C. Wagner, “General Focus Point in the MSSM,” arXiv:1402.1735 [hep-ph].
- [9] K. L. Chan, U. Chattopadhyay and P. Nath, “Naturalness, weak scale supersymmetry and the prospect for the observation of supersymmetry at the Tevatron and at the CERN LHC,” Phys. Rev. D **58** (1998) 096004 [hep-ph/9710473].
- [10] J. L. Feng, K. T. Matchev and T. Moroi, “Focus points and naturalness in supersymmetry,” Phys. Rev. D **61** (2000) 075005 [hep-ph/9909334]; J. L. Feng, K. T. Matchev and D. Sanford, “Focus Point Supersymmetry Redux,” Phys. Rev. D **85** (2012) 075007 [arXiv:1112.3021 [hep-ph]].
- [11] J. L. Feng and D. Sanford, “A Natural 125 GeV Higgs Boson in the MSSM from Focus Point Supersymmetry with A-Terms,” Phys. Rev. D **86** (2012) 055015 [arXiv:1205.2372 [hep-ph]].

- [12] J. Poveda [ATLAS and CMS Collaborations], “Third generation superpartners: Results from ATLAS and CMS,” *Int. J. Mod. Phys. Conf. Ser.* **31**, 1460294 (2014) [arXiv:1402.6253 [hep-ex]].
- [13] M. Carena, A. Freitas and C. E. M. Wagner, “Light Stop Searches at the LHC in Events with One Hard Photon or Jet and Missing Energy,” *JHEP* **0810**, 109 (2008) [arXiv:0808.2298 [hep-ph]].
- [14] A. Menon and D. E. Morrissey, “Higgs Boson Signatures of MSSM Electroweak Baryogenesis,” *Phys. Rev. D* **79**, 115020 (2009) [arXiv:0903.3038 [hep-ph]].
- [15] D. Curtin, P. Jaiswal and P. Meade, “Excluding Electroweak Baryogenesis in the MSSM,” *JHEP* **1208**, 005 (2012) [arXiv:1203.2932 [hep-ph]].
- [16] T. Cohen, D. E. Morrissey and A. Pierce, “Electroweak Baryogenesis and Higgs Signatures,” *Phys. Rev. D* **86**, 013009 (2012) [arXiv:1203.2924 [hep-ph]].
- [17] M. Carena, S. Gori, N. R. Shah, C. E. M. Wagner and L. -T. Wang, “Light Stops, Light Staus and the 125 GeV Higgs,” *JHEP* **1308**, 087 (2013) [arXiv:1303.4414, arXiv:1303.4414 [hep-ph]].
- [18] J. E. Camargo-Molina, B. Garbrecht, B. O’Leary, W. Porod and F. Staub, “Constraining the Natural MSSM through tunneling to color-breaking vacua at zero and non-zero temperature,” arXiv:1405.7376 [hep-ph]; and references therein.
- [19] N. Blinov and D. E. Morrissey, “Vacuum Stability and the MSSM Higgs Mass,” *JHEP* **1403** (2014) 106 [arXiv:1310.4174 [hep-ph]].
- [20] J. M. Frere, D. R. T. Jones and S. Raby, “Fermion Masses and Induction of the Weak Scale by Supergravity,” *Nucl. Phys. B* **222** (1983) 11; L. Alvarez-Gaume, J. Polchinski and M. B. Wise, “Minimal Low-Energy Supergravity,” *Nucl. Phys. B* **221** (1983) 495; J. P. Derendinger and C. A. Savoy, “Quantum Effects and SU(2) x U(1) Breaking in Supergravity Gauge Theories,” *Nucl. Phys. B* **237** (1984) 307; C. Kounnas, A. B. Lahanas, D. V. Nanopoulos and M. Quiros, “Low-Energy Behavior of Realistic Locally Supersymmetric Grand Unified Theories,” *Nucl. Phys. B* **236** (1984) 438.
- [21] A. Kusenko, P. Langacker and G. Segre, “Phase transitions and vacuum tunneling into charge and color breaking minima in the MSSM,” *Phys. Rev. D* **54** (1996) 5824 [hep-ph/9602414]; J. A. Casas, A. Lleyda and C. Munoz, “Strong constraints on the parameter space of the MSSM from charge and color breaking minima,” *Nucl. Phys. B* **471** (1996) 3 [hep-ph/9507294].
- [22] J. S. Lee, M. Carena, J. Ellis, A. Pilaftsis and C. E. M. Wagner, “CPsuperH2.3: an Updated Tool for Phenomenology in the MSSM with Explicit CP Violation,” *Comput. Phys. Commun.* **184**, 1220 (2013) [arXiv:1208.2212 [hep-ph]]; J. S. Lee, M. Carena, J. Ellis, A. Pilaftsis and C. E. M. Wagner, “CPsuperH2.0: an Improved Computational

- Tool for Higgs Phenomenology in the MSSM with Explicit CP Violation,” *Comput. Phys. Commun.* **180**, 312 (2009) [arXiv:0712.2360 [hep-ph]]; J. S. Lee, A. Pilaftsis, M. S. Carena, S. Y. Choi, M. Drees, J. R. Ellis and C. E. M. Wagner, “CPsuperH: A Computational tool for Higgs phenomenology in the minimal supersymmetric standard model with explicit CP violation,” *Comput. Phys. Commun.* **156**, 283 (2004) [hep-ph/0307377].
- [23] R. Barbieri and G. F. Giudice, “ $b \rightarrow s$ gamma decay and supersymmetry,” *Phys. Lett. B* **309**, 86 (1993) [hep-ph/9303270].
 - [24] M. S. Carena, P. H. Chankowski, M. Olechowski, S. Pokorski and C. E. M. Wagner, “Bottom - up approach and supersymmetry breaking,” *Nucl. Phys. B* **491**, 103 (1997) [hep-ph/9612261]; “On the soft supersymmetry breaking parameters in gauge mediated models,” *Nucl. Phys. B* **528**, 3 (1998) [hep-ph/9801376].
 - [25] S. S. AbdusSalam, B. C. Allanach, H. K. Dreiner, J. Ellis, U. Ellwanger, J. Gunion, S. Heinemeyer and M. Kraemer *et al.*, “Benchmark Models, Planes, Lines and Points for Future SUSY Searches at the LHC,” *Eur. Phys. J. C* **71** (2011) 1835 [arXiv:1109.3859 [hep-ph]].
 - [26] A. Brignole, L. E. Ibanez and C. Munoz, “Towards a theory of soft terms for the supersymmetric Standard Model,” *Nucl. Phys. B* **422**, 125 (1994) [Erratum-ibid. B **436**, 747 (1995)] [hep-ph/9308271].
 - [27] D. Horton and G. G. Ross, “Naturalness and Focus Points with Non-Universal Gaugino Masses,” *Nucl. Phys. B* **830** (2010) 221 [arXiv:0908.0857 [hep-ph]].
 - [28] K. Agashe, “Can multi - TeV (top and other) squarks be natural in gauge mediation?,” *Phys. Rev. D* **61** (2000) 115006 [hep-ph/9910497].
 - [29] A. Delgado, G. Nardini and M. Quiros, “The Light Stop Scenario from Gauge Mediation,” *JHEP* **1204** (2012) 137 [arXiv:1201.5164 [hep-ph]].
 - [30] G. Aad *et al.* [ATLAS Collaboration], “Search for direct third-generation squark pair production in final states with missing transverse momentum and two b -jets in $\sqrt{s} = 8$ TeV pp collisions with the ATLAS detector,” *JHEP* **1310**, 189 (2013) [arXiv:1308.2631 [hep-ex]].
 - [31] N. Arkani-Hamed, A. Delgado and G. F. Giudice, “The Well-tempered neutralino,” *Nucl. Phys. B* **741**, 108 (2006) [hep-ph/0601041].
 - [32] J. R. Ellis, A. Ferstl and K. A. Olive, “Exploration of elastic scattering rates for supersymmetric dark matter,” *Phys. Rev. D* **63**, 065016 (2001) [hep-ph/0007113].
 - [33] H. Baer, A. Mustafayev, E. -K. Park and X. Tata, “Target dark matter detection rates in models with a well-tempered neutralino,” *JCAP* **0701**, 017 (2007) [hep-ph/0611387].

- [34] C. Cheung, L. J. Hall, D. Pinner and J. T. Ruderman, “Prospects and Blind Spots for Neutralino Dark Matter,” JHEP **1305**, 100 (2013) [arXiv:1211.4873 [hep-ph]].
- [35] P. Huang and C. E. M. Wagner, “Blind Spots for neutralino Dark Matter in the MSSM with an intermediate m_A ,” arXiv:1404.0392 [hep-ph].